Molecular Biology of the Cell
Vol. 14, 4605–4617, November 2003

Rapid Microtubule-dependent Induction of Neurite-like Extensions in NIH 3T3 Fibroblasts by Inhibition of ROCK and Cbl

Robin M. Scaife,*†‡ Didier Job,† and Wallace Y. Langdon*

*Department of Pathology, University of Western Australia, Crawley, WA 6009, Australia; and
†Départment de Réponse et Dynamique Cellulaires, Commissariat à l'Energie Atomique, Grenoble, France

Submitted November 18, 2002; Revised June 26, 2003; Accepted July 14, 2003
Monitoring Editor: Ted Salmon

A number of key cellular functions, such as morphological differentiation and cell motility, are closely associated with changes in cytoskeletal dynamics. Many of the principal signaling components involved in actin cytoskeletal dynamics have been identified, and these have been shown to be critically involved in cell motility. In contrast, signaling to microtubules remains relatively uncharacterized, and the importance of signaling pathways in modulation of microtubule dynamics has so far not been established clearly. We report here that the Rho-effector ROCK and the multiadaptor proto-oncoprotein Cbl can profoundly affect the microtubule cytoskeleton. Simultaneous inhibition of these two signaling molecules induces a dramatic rearrangement of the microtubule cytoskeleton into microtubule bundles. The formation of these microtubule bundles, which does not involve signaling by Rac, Cdc42, Crk, phosphatidylinositol 3-kinase, and Abl, is sufficient to induce distinct neurite-like extensions in NIH 3T3 fibroblasts, even in the absence of microfilaments. This novel microtubule-dependent function that promotes neurite-like extensions is not dependent on net changes in microtubule polymerization or stabilization, but rather involves selective elongation and reorganization of microtubules into long bundles.

INTRODUCTION

In light of its involvement in numerous cellular functions, the cytoskeleton is critically required for cell division and motility. The assembly of functionally distinct cytoskeletal structures is governed by a variety of regulatory signals and prominent among these is receptor tyrosine kinase (RTK)-mediated signal input to the actin cytoskeleton. RTK-mediated changes in actin cytoskeletal dynamics are mediated by members of the Rho-GTPases (Hall, 1998). It has been well established that the activation of Rho mediates stress fiber formation, whereas Rac and Cdc42 activation lead to the formation of lamellipodia and filopodia associated with cell spreading and directional motility. These Rac- and Cdc42-induced actin structures are prominent structural features of growth cones of neuronal cells (Schaefer *et al*., 2002; Zhou *et al*., 2002).

In contrast, very little has been established regarding signaling to the microtubule network (Gunderson and Cook, 1999; Hollenbeck, 2001), although these cytoskeletal fibers are also subject to rearrangements after changes in cellular conditions. Effects of activated Rho on microtubules have been reported previously (Cook *et al*., 1998) and these seem to occur by mDia-mediated microtubule stabilization (Palazzo *et al*., 2001). The molecular mechanism of this stabilization remains unknown, and it is not clear whether this actually reflects a direct effect on microtubules. However, Rac-mediated signaling to the microtubule cytoskeleton is suggested by the discovery of direct association between the Rac effector IQGAP and the microtubule "plus-end" CLIPs (Fukata *et al*., 2002). Similarly, it has recently been reported that microtubule-dependent cell polarization and centrosome repositioning involves Cdc42-mediated signaling and association of APC with microtubule plus-ends (Etienne-Manneville and Hall, 2003).

Here, we demonstrate that the Rho effector ROCK and the multiadaptor proto-oncoprotein Cbl can dramatically affect the microtubule cytoskeleton. ROCK has clearly been implicated in regulation of the actin cytoskeleton because it phosphorylates a number of F-actin–associated targets (Matsui *et al*., 1998; Fukata *et al*., 1999). On the other hand, the biological function of Cbl remained elusive until the discovery of its RING finger-mediated E3 ubiquitin ligase activity (Joazeiro *et al*., 1999). In light of its ability to act as a ubiquitin-conjugating E3-ligase for tyrosine kinases, and its role in *elegans* and *Drosophila* RTK signaling, Cbl has mostly been described as a negative regulator of protein tyrosine kinases (reviewed in Thien and Langdon, 2001). We have previously shown that inhibition of Cbl by expression of a dominant negative construct profoundly enhances Rac-mediated signaling to the actin cytoskeleton, suggesting a role for Cbl as a negative regulator of Rac (Scaife *et al*., 2003). Indeed, we have recently shown that thymocytes from c-Cbl knockout and tyrosine kinase binding (TKB) domain inactivated knockin mice show markedly elevated levels of GTP-bound Rac (Thien *et al*., 2003). In this report, we extend our analysis of Cbl's regulation of the cytoskeleton and find that the simultaneous inhibition of Cbl and ROCK in NIH 3T3 fibroblasts induces microtubule bundles and rapidly leads to the formation of neurite-like extensions. Interestingly, the formation of microtubule-rich extensions in response to ROCK

Article published online ahead of print. Mol. Biol. Cell 10.1091/mbc.E02–11–0739. Article and publication date are available at www.molbiolcell.org/cgi/doi/10.1091/mbc.E02–11–0739.

‡ Corresponding author. E-mail address: rscaife@cyllene.uwa.edu.au.

and Cbl inhibition is independent of both microtubule stabilization and the actin cytoskeleton. Rather, the ROCK and Cbl regulated formation of these structures represents a novel microtubule bundling-dependent function.

MATERIALS AND METHODS

Cell Culture

NIH 3T3 fibroblasts were obtained from American Type Culture Collection (Manassas, VA) and cultured in DMEM (Trace Biochemicals, Noble Park, Australia) containing 10% fetal calf serum (FCS) (Invitrogen, Carlsbad, CA) and 2 mM L-glutamine (Trace Biochemicals) at 37°C and 5% CO_2. PC12 cells were provided by Dr. David Bowtell (Peter Macallum Cancer Institute, Melbourne, Australia) and were cultured at 37°C and 5% CO_2 in DMEM containing 5% FCS (Invitrogen), 10% donor horse serum (Trace Biochemicals), and 2 mM L-glutamine (Trace Biochemicals) supplemented with 20–100 ng/ml nerve growth factor (NGF) (Sigma-Aldrich, St. Louis, MO).

Cells were grown to ~50% confluence before serum starvation for 24 h in DMEM + 0.5% FCS. Serum-starved cells were activated at 37°C with 10 ng/ml platelet-derived growth factor (PDGF) (human recombinant AA homodimer, UBI, Lake Placid, NY, or Invitrogen), 5 μM lysophosphatidate (LPA), or 10% FCS after a 30-min incubation either with dimethyl sulfoxide (DMSO) carrier or with the pharmacological agents Genestein (100 μM; Calbiochem, San Diego, CA), SU6656 (5 μM; Sugen, South San Francisco, CA), LY294002 (30 μM; Sigma-Aldrich), or SCH-51344 (50 μM, provided by Dr. C. Kumar, Schering-Plough Research Institute, Kenilworth, NJ).

Plasmids and Transfections

Constitutively active Rho (L63RhoA), subcloned into pRK-myc, was provided by Alan Hall (University College, London, United Kingdom), whereas enhanced green fluorescent protein chimeras of dominant negative Rac (N17Rac1) and dominant negative Cdc42 (N17), were provided by Dr. Nathalie Morin (CNRS UPR 1086, Montpellier, France). Constitutively active Rho and dominant negative ROCK and Crk were expressed by transient cotransfection of plasmid containing the cDNA coding for L63Rho-A, ROCK-KIDA (Hirose *et al*., 1998), or Crk-SH2* or Crk-SH3*(Tanaka *et al*., 1993) with pcDNA3 plasmid coding for enhanced green fluorescent protein-tagged with a nuclear localization signal (NLS-GFP; provided by Dr. J. Borst, NKI, Amsterdam the Netherlands). pJZenNeo vectors encoding hemagglutinin epitope-tagged c-Cbl cDNAs have been described previously (Andoniou *et al*., 1994). pJZenNeo constructs were electroporated into Ψ2 packaging cells to generate virus particles for infection of NIH 3T3 cells, which were selected with 400 μg/ml active G418 (Invitrogen). All other cDNA constructs were expressed transiently after transfection of cells using FuGENE 6 transfection reagent (Roche Diagnostics, Mannheim, Germany).

Immunofluorescence and Phase Contrast Microscopy

For immunofluorescence microscopy, NIH 3T3 cells were seeded onto coverslips coated with polylysine (0.1 mg/ml) in the presence or absence of 1 μM cytochalasin D, 1 μg/ml nocodazole, 2 μM taxol, 8 μM ML-7 (Calbiochem), and 25 μM Y-27632 (Welfide, Osaka, Japan) before fixation in 4% *p*-formaldehyde/phosphate-buffered saline (PBS). PC12 cells were similarly seed onto glass coverslips but were fixed in 100% methanol at −20°C for 20 min. The fixed cells were then permeabilized for 1 min with 0.2% Triton X-100 in PBS containing 2.5 mg/ml bovine serum albumin (BSA). Coverslips were rinsed with PBS and incubated for 60 min, with 0.5 μg/ml tetramethylrhodamine B isothiocyanate (TRITC)-phalloidin (Sigma-Aldrich) and anti-tubulin antibodies (7.5 μg/ml, monoclonal antibody T-4026; Sigma-Aldrich) at 37°C for 60 min in PBS containing 2.5 mg/ml BSA. After a PBS wash, the coverslips were incubated with 5 μg/ml biotin-SP–conjugated goat anti-mouse (115-065-003; Jackson Immunoresearch Laboratories, West Grove, PA) at 37°C for 60 min in PBS containing 2.5 mg/ml BSA. Biotin-labeled antigen–antibody complexes were then visualized by incubation for 60 min with PBS containing 2.5 mg/ml BSA and 2 μg/ml Alexa 488 conjugated streptavidin (Molecular Probes, Eugene, OR), and nuclei were stained with Hoescht 33342. For detection of Glu-tubulin, cells were stained using this same protocol, except that TRITC-phalloidin was replaced with rabbit polyclonal anti-Glu antibodies (Paturle-Lafanechere *et al*., 1994) that were detected using Alexa 546-conjugated goat anti-rabbit antibodies (Molecular Probes). Acetylated tubulin was detected using 1/2,000 diluted monoclonal antibody 6-11b-1 (Sigma-Aldrich), followed by Cy3-conjugated donkey anti-mouse antibody (715-165-150; Jackson Immunoresearch Laboratories). In the case of cells transfected with green fluorescent protein (GFP) constructs, the anti-tubulin antibody was visualized by incubation of the coverslips with Alexa 546-conjugated anti-mouse secondary antibodies (A11003; Molecular Probes).

After a PBS rinse, coverslips were mounted with SlowFade Light Antifade reagent (Molecular Probes). Images of representative fields were obtained with Comos and Confocal Assistant software (Bio-Rad, Hercules, CA) after capture on a Nikon Diaphot 300 microscope equipped for UV laser scanning confocal microscopy (MRC 1000/1024; Bio-Rad).

Phase contrast images of cells were obtained using either a Leitz Labovert FS (6.3× objective lens) or an Olympus T-41 (20× objective lens) microscope, and single-length measurements were performed using Optimas software processing of digital microscope images. Average distance measurements from the nucleus to the cell boundary (following the curvature of extensions, where applicable) were obtained using Optimas software after capture of anti-tubulin confocal immunofluorescence images (average of 27 cells/image) using a 20× objective lens.

Cell Lysis, Fractionation, and Western Blotting

Cells were washed with PBS and total lysates were obtained by addition of 37.5 mM HEPES buffer (pH 7.4) containing 112.5 mM NaCl, 0.75% Triton X-100, 0.75% sodium deoxycholate, 1% SDS, 10% glycerol, 1 mM $MgCl_2$, 0.75 mM EDTA, and protease inhibitors at 100°C. Cytoskeletal fractions were obtained after extraction of cytosolic proteins by a 1-min incubation of the cells with 80 mM PIPES (pH 6.7), 1 mM EGTA, 1 mM $MgCl_2$, 10% glycerol, 0.3% Triton X-100, 5% polyethylene glycol, and protease inhibitors at 37°C. After sonication, aliquots of total cell lysates and cytoskeletal fractions were subjected to SDS-PAGE and transferred onto nitrocellulose membranes (Amersham Biosciences, Piscataway, NJ). Membranes were blocked with 10% nonfat milk (Carnation, Melbourne, Australia), 5% BSA (Roch Diagnostics) in Tris-buffered saline containing 0.5% Tween 20, and probed with antibodies directed against β-tubulin (clone TUB2.1; Sigma-Aldrich), followed by horseradish peroxidase-conjugated secondary antibody (Silenus, Melbourne, Australia). Antigen was then visualized by chemiluminescence (Amersham Biosciences) using Hyperfilm MP (Amersham Biosciences).

RESULTS

Involvement of Cbl in RTK-Activation–dependent Changes in Cell Morphology

Growth factor-mediated induction of receptor tyrosine kinase signaling pathways can result in rapid and marked changes in cell morphology. For example, exposure of serum-starved NIH 3T3 fibroblasts to PDGF rapidly leads to a minor alteration in cell morphology, characterized by a partial collapse of the original cell shape (Figure 1A, panels 1–3). In contrast, we found that PDGF treatment of cells expressing 388-Cbl (a dominant negative TKB domain construct [Scaife *et al*., 2003] of c-Cbl) induced a transient, but pronounced, rounding of the cell bodies concomitant with the appearance of long cytoplasmic extensions (Figure 1A, panels 4–6). This effect of 388-Cbl was specific for growth factor-mediated activation of RTKs because treatment of serum-starved 388-Cbl–expressing cells with either FCS or LPA did not elicit a change in cell morphology (Figure 1B). Furthermore, although the tyrosine kinase inhibitor genestein and the Src inhibitor SU-6656 blocked the effect of 388-Cbl on PDGF-induced changes in cell morphology, the phosphatidylinositol 3-kinase (PI 3-kinase) inhibitor LY-294002 and the Rac signal inhibitor SCH-51344 had no effect (Figure 1B). Similarly, transient expression of dominant negative Rac1 or Cdc42 constructs did not block the PDGF-induced morphological change (our unpublished data). Hence, this response to PDGF requires the activity of protein tyrosine kinases, such as Src, whereas PI 3-kinase-, Rac-, and Cdc42-activated pathways do not seem to be involved.

RTK-Activation–dependent Changes in Cell Morphology Involve Microtubule Reorganization and Signaling by Rho

Because the cytoskeleton is considered a principal determinant of cell morphology, we examined whether cytoskeletal rearrangements could underlie the profound morphological changes induced by PDGF and dominant negative Cbl. We found that staining the 388-Cbl expressing cells with anti-tubulin antibody revealed a striking cytoskeletal change after PDGF activation that resulted in the appearance of microtubule-rich extensions emanating from the cell body

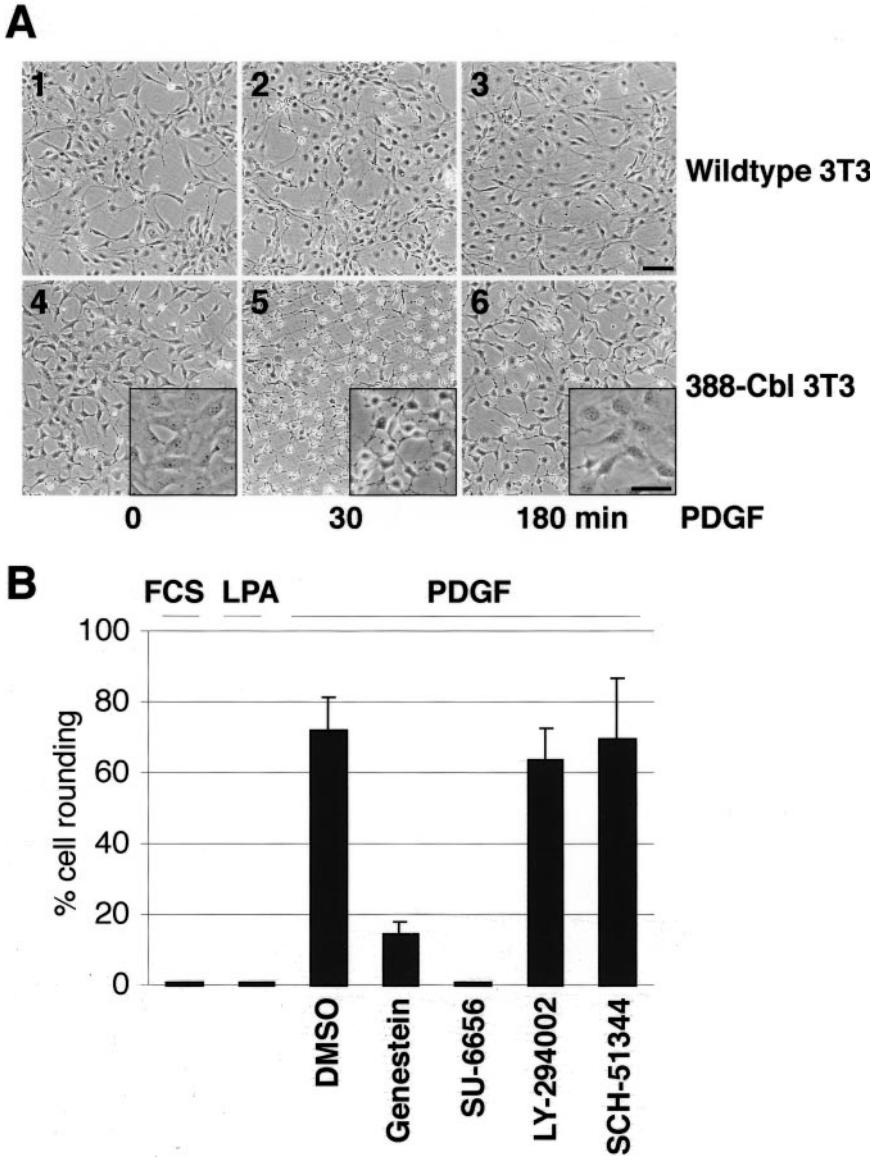

Figure 1. Involvement of Cbl in RTK-activation–dependent changes in cell morphology. (A) Serum-starved wild-type (1–3) and 388-Cbl–expressing (4–6) NIH 3T3 cells were either left untreated (1 and 4) or were treated with PDGF for 30 min (2 and 5) or 180 min (3 and 6). Phase contrast images of the cells were collected at the indicated time points. The panel insets represent higher magnification views. Bar, 100 μm. (B) After a 30-min incubation with either no addition, DMSO, genestein, SU 6656, LY 294002, or SCH-51344. Serum-starved 388-Cbl–expressing NIH 3T3 cells were treated for a further 30 min with FCS, LPA, or PDGF, as indicated. Phase contrast images of the cells were collected at this time point, and the percentage of cells that had undergone extensive cell rounding was determined.

(Figure 2A, panels 1 and 2). We therefore wished to examine whether microtubules are required for the appearance of these extensions. Brief exposure of cells to nocodazole, before PDGF activation, resulted in depolymerization of microtubules and inhibition of the formation of extensions (Figure 2A, 3 and 4).

It is well established that members of the Rho-family of GTPases are key mediators of signal transduction from RTKs to the actin cytoskeleton (Hall, 1998), and there is increasing evidence that RhoA is also involved in the regulation of microtubule dynamics (Cook *et al*., 1998; Wittman and Waterman-Storer, 2001). Indeed, changes in cell morphology in response to PDGF receptor activation are thought to be due to transient down-regulation of Rho (Sander *et al*., 1999). Therefore, by expressing a constitutively active form of RhoA in 388-Cbl cells, we could assess whether its down-regulation is involved in PDGF-induced changes in cell morphology and microtubule reorganization. We found that expression of constitutively active RhoA fully blocked the PDGF-induced extensions (Figure 2B), suggesting that the formation of extensions requires the down-regulation of RhoA.

ROCK Inactivation Induces Changes in Cell Morphology Identical to RTK-induced Changes

The effects of Rho on signaling to the microtubule cytoskeleton could be mediated by effectors such as the adaptor protein mDia or the Rho-activated kinase ROCK (Aspenstrom, 1999). Although mDia has indeed been demonstrated to associate with microtubules, its stabilizing effect on microtubules is not associated with pronounced changes in microtubule organization (Palazzo *et al*., 2001) and hence is unlikely to be involved in the marked microtubule reorganization seen in PDGF-treated 388-Cbl cells. We therefore assayed whether inhibition of the Rho effector p160ROCK could underlie the PDGF-induced induction of extensions and microtubule bundles. We found that treatment of 388-Cbl cells, and to much lesser extent wild-type NIH 3T3 cells, with the synthetic ROCK inhibitor Y-27632 resulted in pro-

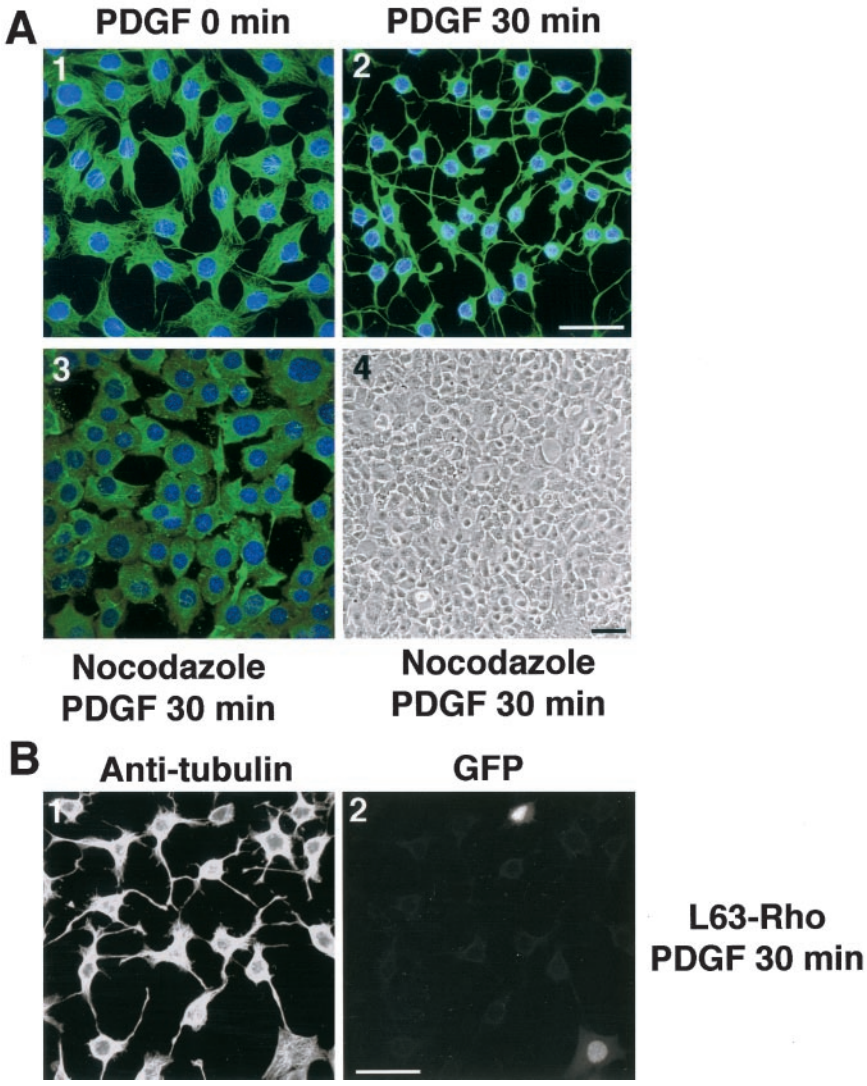

Figure 2. RTK-activation–dependent changes in cell morphology involves microtubule reorganization and signaling by Rho. (A) Serum-starved 388-Cbl–expressing NIH 3T3 cells were left untreated (1) or were either treated with PDGF (30 min) (2) or with nocodazole (20 min) followed by PDGF (30 min) (3 and 4). Cells were then either observed directly by phase contrast microscopy (4) or were stained with anti-tubulin antibody and Hoescht and imaged by confocal immunofluorescence microscopy (1–3). Bars, 50 μm. (B) 388-Cbl–expressing NIH 3T3 cells were cotransfected with L63RhoA and NLS-GFP cDNA. After serum starvation, the cells were treated with PDGF for 30 min and anti-tubulin (1) and GFP fluorescence (2) images were captured by confocal microscopy. Bar, 50 μm.

nounced formation of microtubule-rich extensions that were indistinguishable from those formed by PDGF-activated cells (Figure 3A, 1, 2, 4, and 5). This effect of Y-27632 on the cell morphology and microtubule cytoskeleton does not seem to be a secondary consequence of ROCK inhibition-induced stress fiber loss because disassembly of stress fibers by the myosin light-chain kinase inhibitor ML-7 induced cell collapse without concomitant formation of microtubule-rich extensions (Figure 3A, 3 and 6).

To examine whether the Y-27632-induced extensions represent unique structures generated by lengthening beyond the boundaries of untreated cells, we examined the morphological response of a group of cells by time-lapse imaging and measurement of cell dimensions. 388-Cbl–expressing cells that had been allowed to adhere to the culture substrate for 24 h were imaged by phase contrast microscopy before (0 min) and after exposure (60 min) to Y-27632 (Figure 3B). Clearly, treatment of these cells with the ROCK inhibitor resulted in the formation of distinct protrusions that extended well beyond the original boundaries of the cells.

The critical involvement of ROCK in this microtubule-based cellular response was further confirmed by expression of a dominant negative p160ROCK cDNA construct (ROCK-KIDA) (Hirose *et al*., 1998). Indeed, expression of this construct similarly resulted in a pronounced change in cell morphology involving the appearance of microtubule-rich extensions (Figure 3C).

Inhibition of ROCK Induces Polarity and Microtubule-rich Extensions in 388-Cbl–expressing NIH 3T3 Fibroblasts

The appearance of microtubule-rich extensions after ROCK inhibition is likely to be due to induction of cell polarization and elongation. To assay to what extent preexisting cell polarity and morphological features might be involved in the formation of the cytoplasmic extensions, we examined the response of freshly plated cells. We used both time-lapse phase contrast microscopy of live cells (Figure 4A), and immunofluorescence microscopy (Figure 4B), to examine the effect of ROCK inhibition on freshly replated cells. The freshly replated cells are spherical at the start of the analyses, and there is no evidence of preexisting morphological polarity (Figure 4, A, 1 and 5; and B, 1 and 4). In the presence of the ROCK inhibitor, freshly plated 388-Cbl cells rapidly (30 min) formed cytoplasmic protrusions (Figure 4A, 6),

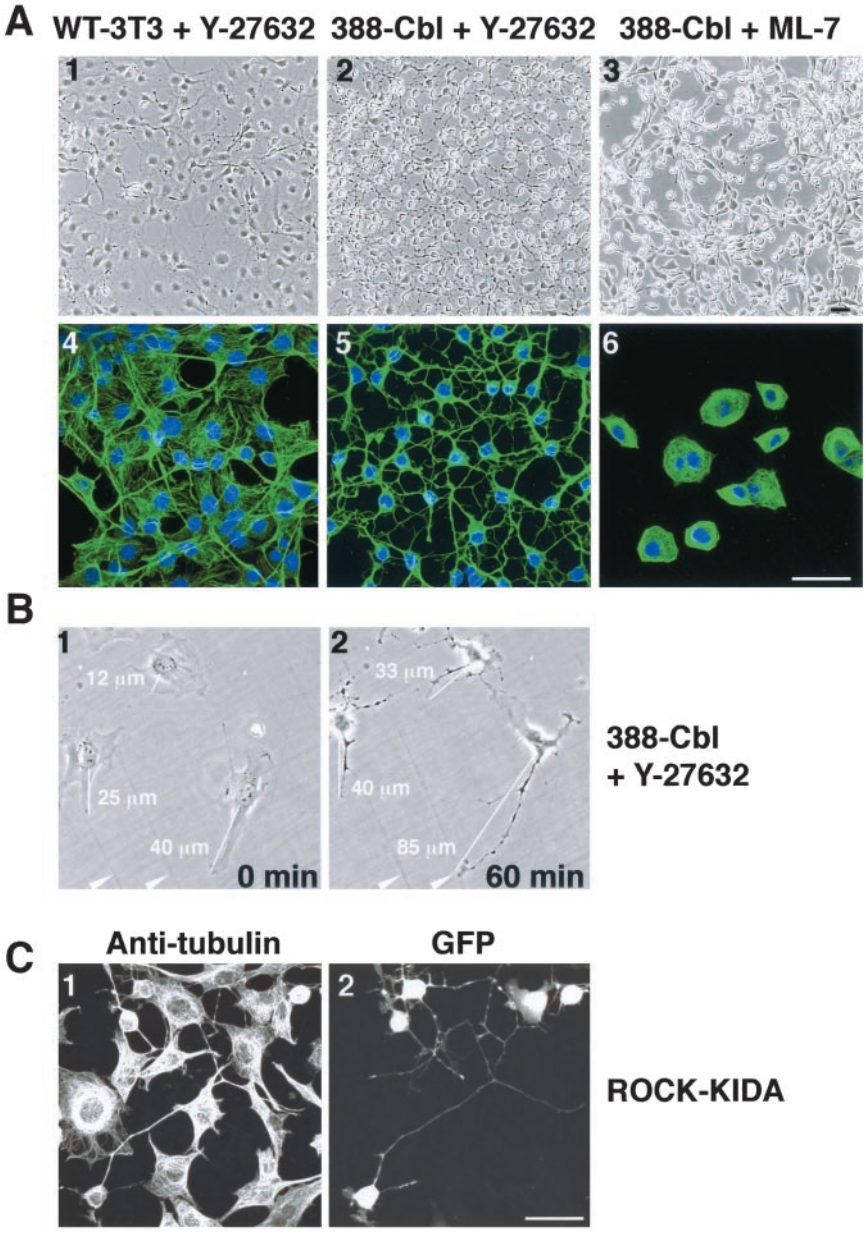

Figure 3. ROCK inactivation induces changes in cell morphology identical to RTK-induced changes. (A) Phase contrast images (1–3) and confocal immunofluorescence of anti-tubulin antibody and Hoescht staining (4–6) of serum-starved wild-type (1 and 4) and 388-Cbl–expressing NIH 3T3 cells (2, 3, 5, and 6) were taken after a 30-min treatment with Y-27632 (1, 2, 4, and 5) or ML-7 (3 and 6). Bar, 50 μm. (B) Phase contrast images were taken of a group of 388-Cbl–expressing cells before (0 min) and after (60 min) of treatment with Y-27632. The distances represented by the white lines are indicated numerically, and two positional markers are indicated by the arrowheads. (C) After transient cotransfection of 388-Cbl–expressing cells with ROCK-KIDA and NLS-GFP–expressing plasmids, anti-tubulin antibody (1) and GFP staining (2) were imaged by confocal immunofluorescence microscopy. Bar, 50 μm.

followed by elongation of these protrusions into long cytoplasmic extensions within 3 h of Y-27632 addition to the culture medium (Figure 4A, 7 and 8). This extensive cytoplasmic elongation and branching in response to ROCK inhibition was accompanied by formation of microtubule-rich bundles in the extensions (Figure 4B, 6). Most remarkably, after prolonged incubation (20 h) with the ROCK inhibitor, these cells lost all resemblance to their normal morphology and formed long, microtubule-rich extensions (Figure 5A, 1 and 2) that resemble the overall morphology of neuritic extensions, such as those formed by NGF-treated PC12 cells (Figure 5A, 3 and 4).

The pharmacologically induced cytoplasmic extensions are comprised of tightly packed parallel arrays or bundles of microtubules (Figure 5B, 2). Enrichment of F-actin at the tips of the Y-27632–induced extensions was frequently observed (Figures 4 and 5), and this is reminiscent of lamellipodial and filopodial F-actin in neuronal growth cones (Da Silva and Dotti, 2002). These findings support the notion that the cytoskeletal and morphological changes in Y-27632–treated 388-Cbl–expressing fibroblasts may mirror some of the changes that occur during neuritogenesis.

Induction of Extensions Is Independent of Signaling by Rac, Cdc42, Crk, PI 3-kinase, and Abl

In light of their effects on lamellipodia and filopodia formation, Rac and Cdc42 are thought to be required for cell polarization and formation of neurite-like processes (Da Silva and Dotti, 2002). We therefore assayed for the involvement of Rac and Cdc42 in the formation of cytoplasmic extensions after ROCK inhibition. However, expression of dominant negative Rac or dominant negative Cdc42 had no effect on the formation of these microtubule

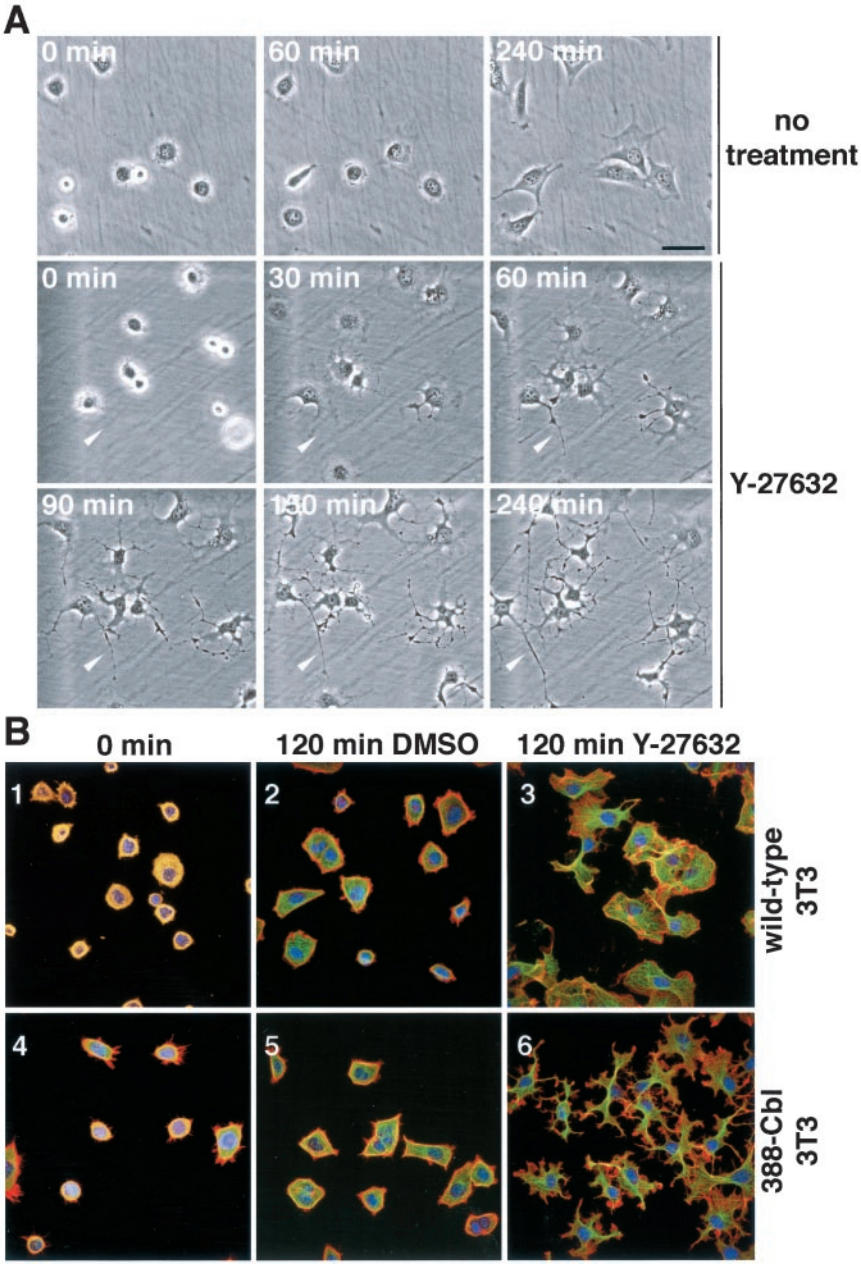

Figure 4. Inhibition of ROCK induces polarity and microtubule-rich extensions in freshly plated 388-Cbl–expressing NIH 3T3 fibroblasts. (A) Phase contrast microscopy images of freshly plated 388-Cbl–expressing cells were collected during incubation in the absence (1–3) or presence of Y-27632 (4–9). The position of a cytoplasmic extension has been indicated by the arrowhead. Bar, 50 μm. (B) Confocal immunofluorescence microscopy images of TRITC-phalloidin (red), anti-tubulin antibody (green), and Hoescht (blue) staining of wild-type (1–3) and 388-Cbl–expressing NIH 3T3 cells (4–6) were collected 30 min after replating (1 and 4), or after an additional 120 min of incubation in the absence (2 and 5) or presence of Y-27632 (3 and 6). Bar, 50 μm.

extensions (Figure 6, 1, 2, 4, and 5). The adaptor protein Crk has been reported to mediate some of the effects of ROCK on the actin cytoskeleton (Tsuji *et al*., 2002). However, expression of dominant negative Crk cDNA constructs with either SH3 (Figure 6, 3 and 6) or SH2 domain (our unpublished data) mutations did not abolish this response to ROCK inhibition. Thus, Crk does not seem to be involved in Y-27632–mediated induction of extensions. PI 3-kinase and the Abl protein tyrosine kinase have also been implicated in regulation of the actin cytoskeleton (Rodriguez-Viciana *et al*., 1997) and the formation of cellular extensions (Woodring *et al*., 2002). However, pharmacological inhibitors of these signaling molecules (by LY-294002 and STI-571, respectively), as well as other tyrosine kinase inhibitors (genestein, PP2, and SU-6656) did not abolish the formation of extensions in response to ROCK inhibition (our unpublished data).

Requirement of Microtubules, but Not Microfilaments, for the Formation of Extensions

Cell spreading and motility are thought to result from the Rac- and Cdc42-mediated assembly of microfilament-based lamellipodia and filopodia (Nobes and Hall, 1999). However, our results indicate that Rac and Cdc42 are not required for the rapid formation of extensions. This suggests that formation of these ROCK inhibition-induced extensions does not require assembly of microfilaments into lamellipodia or filopodia. We therefore assayed whether the actin cytoskeleton is indeed even involved in the ROCK regulated formation of extensions. Consistent with our results using

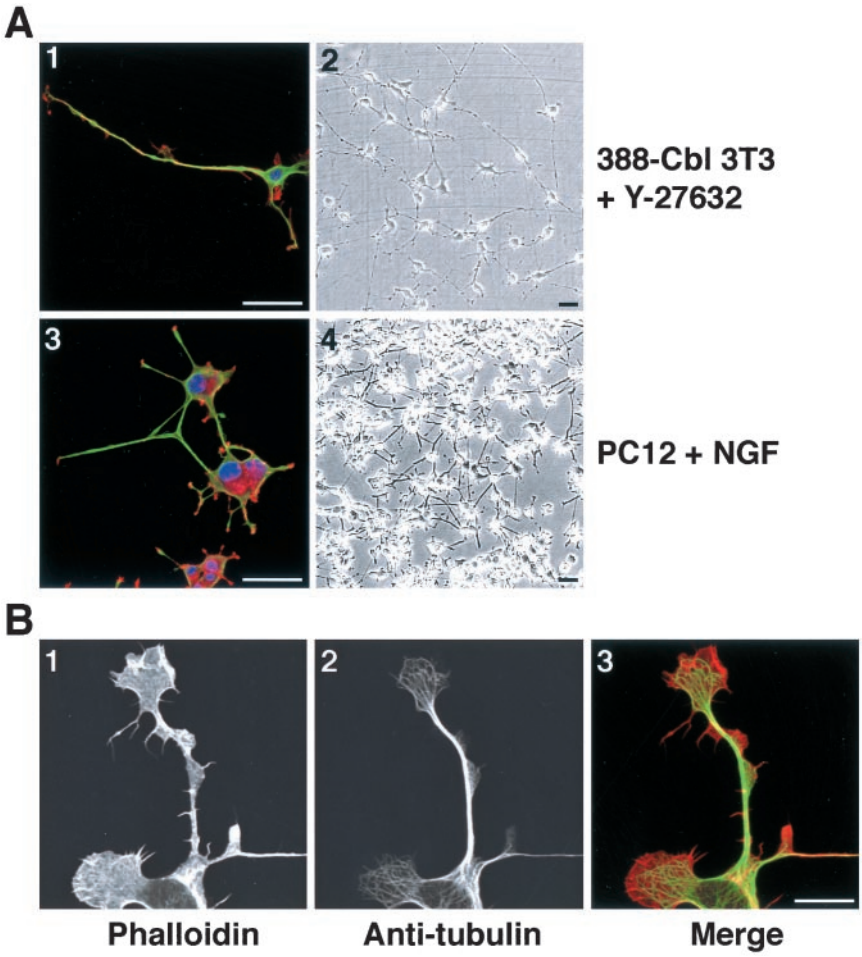

Figure 5. Inhibition of ROCK induces polarity and extensions in freshly plated 388-Cbl–expressing NIH 3T3 fibroblasts. (A) Confocal immunofluorescence microscopy images of TRITC-phalloidin (red), anti-tubulin antibody (green), and Hoescht (blue) staining (1 and 3), and phase contrast images (2 and 4) were collected 20 h after replating of 388-Cbl–expressing NIH 3T3 cells in the presence of Y-27632 (1 and 2), or 3 d after plating of PC12 cells in the presence of NGF (3 and 4). Bar, 50 μm. (B) Confocal immunofluorescence microscopy images of TRITC-phalloidin (1), anti-tubulin antibody (2) of 388-Cbl–expressing NIH 3T3 cells were collected 6 h after replating in the presence of Y-27632. A merged image of the TRITC-phalloidin and anti-tubulin signals is shown in 3. Bar, 12.5 μm.

dominant negative Rac and Cdc42, we found that treatment of 388-Cbl–expressing cells with the microfilament disassembling drug cytochalasin D did not block the formation of extensions after ROCK inhibition by Y-27632 (Figure 7B, 1 and 2).

As was shown in Figures 4 and 5, the addition of Y-27632 to spreading cells is accompanied by extensive reorganization of the microtubule cytoskeleton. This suggests that microtubules may play an important role in the formation of the extensions. Indeed, we found that cells treated with the microtubule depolymerizing drug nocodazole failed to form discrete extensions after exposure to Y-27632 (Figure 7, A, and B, 3 and 4), although the ROCK inhibitor did have a modest effect on overall cell morphology. This indicates that the formation of extensions in response to ROCK inhibition is primarily due to modulation of the microtubule network.

To further examine the involvement of microtubules, we treated cells with the microtubule-stabilizing drug taxol. In control cells, this treatment resulted in numerous densely packed perinuclear microtubules (Figure 7B, 5). However, addition of the ROCK inhibitor to taxol-treated cells resulted in the formation of distinct cytoplasmic protrusions (Figure 7A) that were rich in microtubules (Figure 7B, 6). These results suggest that ROCK inhibition leads to the formation of protrusions by induction of microtubule reorganization into bundles. Although inhibition of microtubule dynamics by taxol did not prevent the bundling of microtubules into cytoplasmic extensions, the presence of taxol seemed to significantly reduce the length of the extensions. To clearly determines whether microtubule dynamics are required for elongation of the Y-27632–induced extensions, we performed a quantitative analysis of extension elongation. From measurements of the maximal distance of the cell boundary to the cell nucleus, it is clear that theY-27632–treated cells undergo a pronounced and steady rate of elongation by de novo formation of cytoplasmic extensions. Interestingly, although cytochalasin had a minimal effect on the elongation of the extensions, treatment of the cells with taxol prevented the pronounced elongation, after an initial burst of extension formation by bundling of the taxol-stabilized microtubules (Figure 7C). These results indicate that the formation of the long cytoplasmic extensions is a multicomponent process, involving both microtubule reorganization into bundles and microtubule dynamics-dependent elongation of the bundles.

The importance of microtubule reorganization, rather than increased net microtubule polymerization, in the Y-27632–induced formation of cytoplasmic extensions was further probed by biochemical assay of microtubule polymerization. Unlike taxol, which greatly induces tubulin polymerization, we found that Y-27632 treatment of the 388-Cbl–expressing cells did not significantly increase the mass of tubulin polymer (Figure 7D). The absence of a significant increase in tubulin polymerization by Y-27632 further highlights the importance of microtubule reorganization into bundles and/or changes in microtubule dynamics, rather

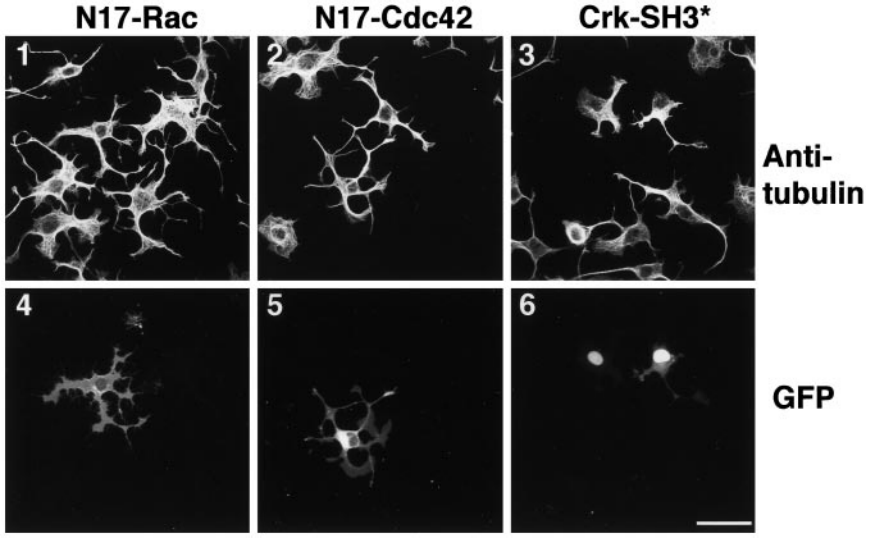

Figure 6. Induction of extensions is independent of signaling by Rac, Cdc42, and Crk. After transfection with GFP-N17Rac1 (1 and 4), GFP-N17Cdc42 (2 and 5) or cotransfection with a Crk SH3 domain mutant (Crk-SH3*) and NLS-GFP (3 and 6), 388-Cbl–expressing cells were replated for 4 h in the presence of Y-27632. Anti-tubulin antibody (1–3) and GFP staining (4–6) was then determined by confocal immunofluorescence microscopy. Bar, 50 μm.

than increased net polymerization, in the induction and elongation of extensions.

Microtubule Bundles Formed by ROCK Inhibition Are Enriched in Detyrosinated Tubulin

Rho-mediated polarized assembly of microtubule arrays in motile fibroblasts has been correlated with induction of stable detyrosinated ("Glu") microtubules (Cook *et al*., 1998). We therefore examined whether a similar mechanism of microtubule stabilization might be involved in the Y-27632–induced formation of cytoplasmic extensions in 388-Cbl–expressing cells. After 2 h of ROCK inhibition, immunofluorescent staining of cells with anti-Glu-tubulin and anti-β-tubulin antibodies revealed that the initial induction of cell polarity and microtubule bundling by Y-27632 was not accompanied by the formation of Glu-microtubules (Figure 8, 1 and 2). However, the extensive microtubule bundling and formation of long extensions that results from prolonged exposure to Y-27632 did result in a significant accumulation of Glu-tubulin in the cytoplasmic extensions (Figure 8, 3 and 4).

Hence, these results indicate that generation of stable Glu-microtubules is not involved in the induction of microtubule bundles and cell polarization, although the highly ordered microtubule bundles do eventually become enriched in Glu-tubulin.

Microtubule Bundles Formed by ROCK Inhibition Share Key Properties of Neuritic Microtubules

In neuronal cells, the formation of neurites coincides with tubulin acetylation and stabilization of microtubule bundles (Lim *et al*., 1989). We therefore tested whether the microtubule bundles formed by ROCK inhibition share these key properties of neuritic microtubules. After ROCK inhibition, immunofluorescent staining of cells with anti-acetylated-tubulin and anti-β-tubulin antibodies revealed that the pronounced microtubule bundling by Y-27632 was indeed accompanied by an accumulation of acetylated tubulin in the cytoplasmic extensions (Figure 9A, 2). This is strikingly similar to the accumulation of acetylated tubulin in the NGF-induced neurites of PC12 cells (Figure 9A, 3). We next investigated whether the pronounced microtubule bundling by Y-27632 could also result in microtubule stabilization. Microtubule stabilization was assayed in terms of the resistance of microtubule polymers to nocodazole-induced depolymerization. Although incubation of untreated 388-Cbl cells with 1 μM nocodazole fully depolymerized all the microtubules (Figure 9B, 1 and 2), we found that the long microtubule bundles that form after prolonged exposure of these cells to Y-27632 are relatively refractory to depolymerization by nocodazole (Figure 9B, 3 and 4).

DISCUSSION

We have demonstrated that NIH 3T3 fibroblasts can be induced to form long cytoplasmic extensions and surprisingly, the formation of these extensions does not directly involve the actin cytoskeleton. Rather, a pronounced rearrangement of microtubules underlies the formation of these extensions. This rearrangement of microtubules into bundles occurs most markedly after PDGF activation, or ROCK inhibition, in NIH 3T3 cells expressing a dominant negative form of Cbl. This phenomena also occurs (albeit to a much lesser extent) with wild-type 3T3 fibroblasts, whereby ROCK inhibition has been reported to similarly induce "neurite-like processes" (Hirose *et al*., 1998). Although these processes indeed bear a degree of resemblance to neurites in terms of geometry and cytoskeletal organization, it remains to be seen to what extent the rapid Y-27632–mediated formation of these neurite-like extensions in fibroblasts and neuronal cells parallels differentiation-induced neuritogenesis (Da Silva and Dotti, 2002).

It has been well established that actin cytoskeletal dynamics are critically involved in cell motility, which is closely associated with cell polarization and the formation of leading edge, F-actin–rich lamellipodia and filopodia. The formation of these structures is particularly clear at the neuritic growth cones of cultured neuronal cells (Schaefer *et al*., 2002; Zhou *et al*., 2002). Furthermore, biological inhibitors of neurite extension have been demonstrated to induce disassembly of actin-rich structures of the growth cone (Luo, 2000).

We have determined that 388-Cbl–expressing NIH 3T3 fibroblasts can be induced to form long cytoplasmic extensions in response to ROCK inhibition. These extensions are morphologically similar to the neurites formed by differentiating neuronal cells, although the kinetics of their formation is very different. The pharmacological induction of ex-

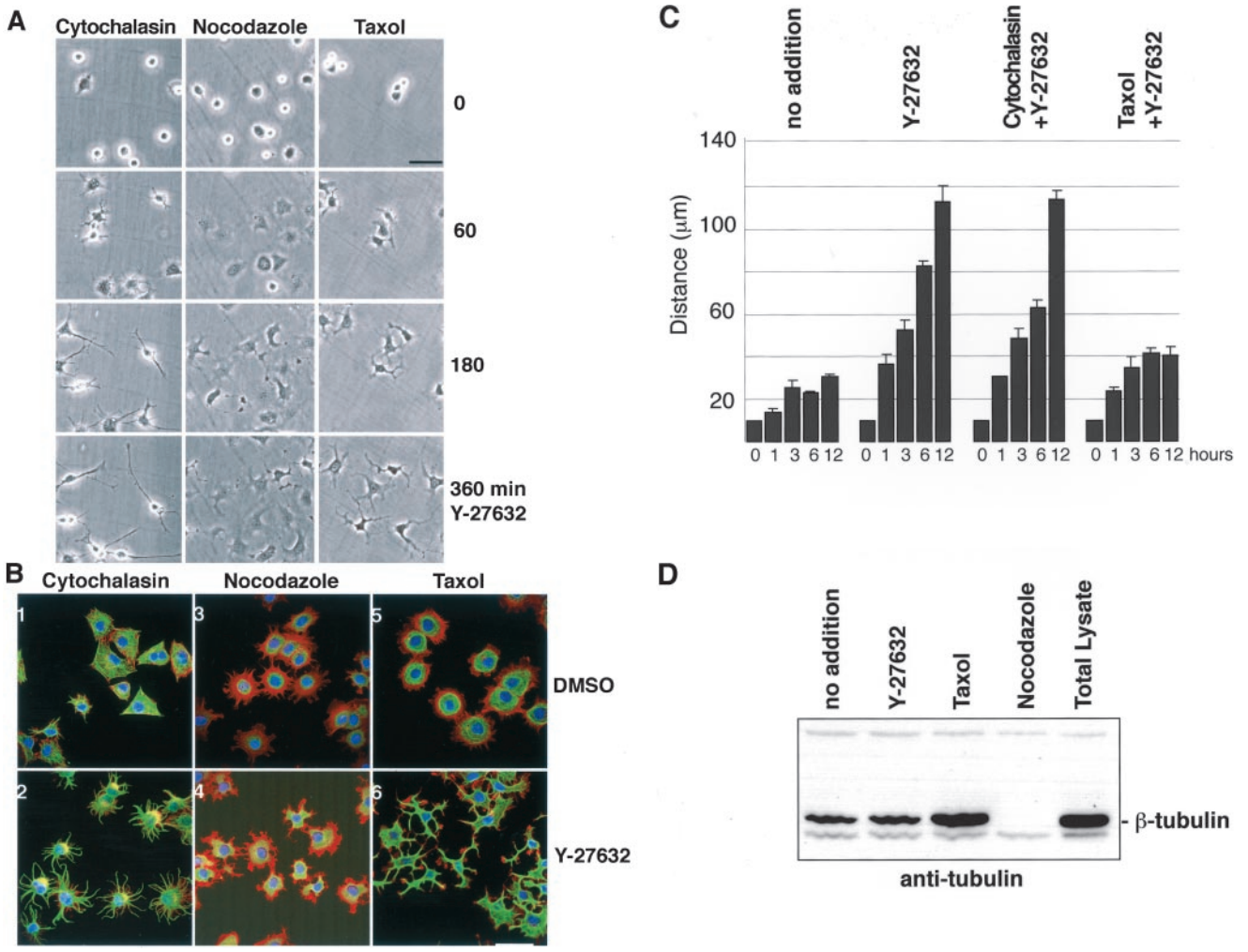

Figure 7. Requirement of microtubules, but not microfilaments, for the formation of extensions. (A) After replating of 388-Cbl–expressing cells for 30 min in the presence of cytochalasin D, nocodazole, or taxol, phase contrast images were collected at 0, 60, 180, and 360 min of addition of Y-27632 to the culture media. Bar, 50 μm. (B) 388-Cbl–expressing cells were replated for 30 min in the presence of cytochalasin D (1 and 2), nocodazole (3 and 4), or taxol (5 and 6). Confocal immunofluorescence microscopy images of phalloidin (red), anti-tubulin antibody (green), and Hoescht (blue) staining of 388-Cbl were then collected after a 4-h incubation with DMSO (1, 3, and 5) or Y-27632 (2, 4, and 6). Bar, 50 μm. (C) 388-Cbl–expressing cells were replated in the absence (no addition) or presence of Y-27632, Y-27632 plus cytochalasin D, and Y-27632 plus taxol. Median maximal distances from the cell boundary to the nucleus were obtained from separate triplicate anti-tubulin immunofluorescence images as described in MATERIALS AND METHODS. Average values and standard deviations are indicated for samples taken at 0, 1, 3, 6, and 12 h of adhesion to the culture substrate after replating. (D) 388-Cbl–expressing cells were replated for 6 h either with no drug treatment (lanes 1 and 5), Y-27632 (lane 2), taxol (lane 3), or nocodazole (for the final 60 min, lane 4), and microtubule cytoskeleton fractions (lanes 1–4) or total cell lysates (lane 5) were probed with anti-tubulin antibody after SDS-PAGE and Western blot.

tensions in NIH 3T3 cells occurs within minutes, and extensions approaching nearly millimeter lengths arise after overnight treatment. In contrast, several days are required to achieve significant neurite formation by neuronal cells exposed to differentiation-inducing factors. Similar to neuronal growth cones, the ends of the neurite-like extensions of NIH 3T3 fibroblasts contain distinct F-actin–based structures. However, because formation of these extensions is not abolished by F-actin disassembly, the leading edge lamellipodia or filopodia may be primarily involved in the formation and/or pathfinding function of the growth cone. Interestingly, this is similar to the previously reported F-actin–independent formation of neurites by neuronal cells (Marsh and Letourneau, 1984) and further supports the notion that with neuronal cells the actin cytoskeleton is similarly involved in growth cone dynamics and steering rather than in neurite extension (Zhou *et al*., 2002).

Formation of extensions, even after the disassembly of F-actin by cytochalasin D treatment, suggested that their formation occur by an F-actin–independent mechanism. The crucial role of microtubules, and not F-actin, was therefore confirmed by treatment with nocodazole, which abolished the formation of the extensions in fibroblasts. This seems analogous to the inhibitory effect of nocodazole on cell polarization induced by ROCK inhibition (Omelchenko *et al*., 2002). However, the inhibition of cell polarization by nocodazole is difficult to interpret because microtubule depolymerization is known to induce Rho-GEF–mediated forma-

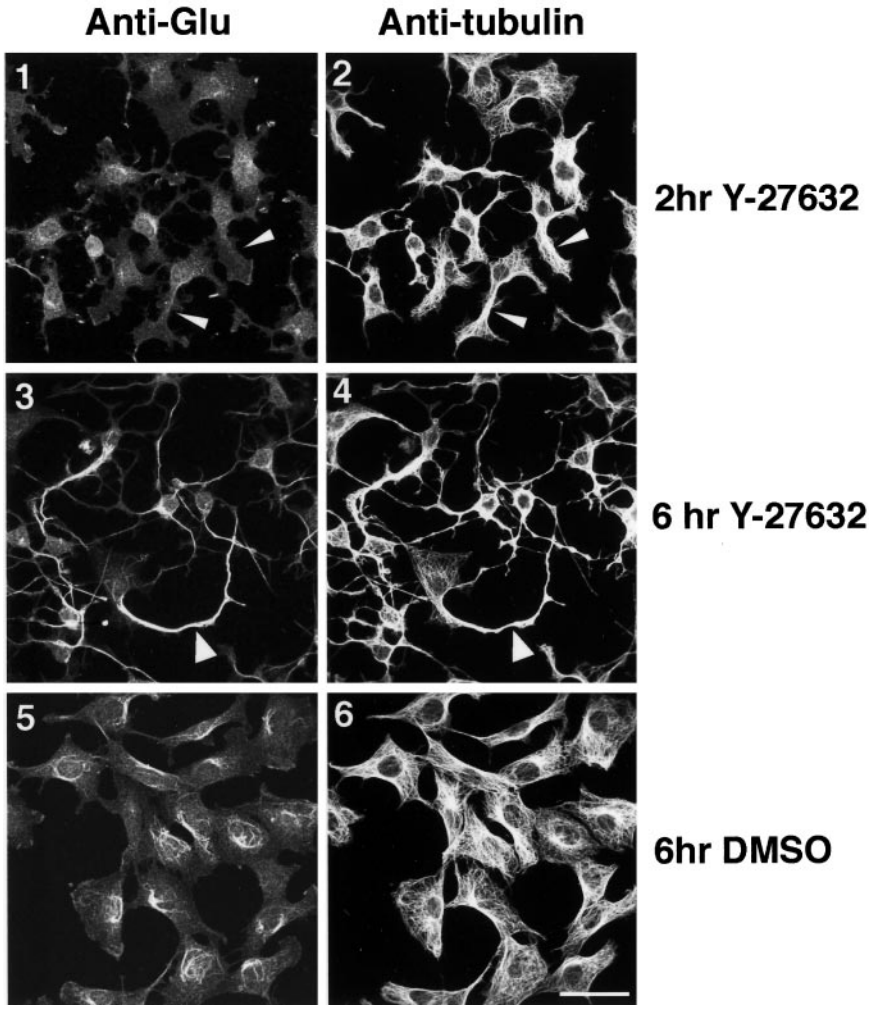

Figure 8. Microtubule bundles formed by ROCK inhibition are enriched in detyrosinated tubulin. Confocal immunofluorescence microscopy images of anti-Glu-tubulin (1, 3, and 5) and anti-β-tubulin (2, 4, and 6) staining of 388-Cbl–expressing cells were collected after 2 h (1 and 2) and after 6 h (3–6) of replating in the presence (3 and 4) and absence (5 and 6) of Y-27632. Non-Glu– and Glu-tubulin–containing microtubule bundles are indicated by narrow and wide arrowheads, respectively. Bar, 50 μm.

tion of stress fibers (Krendel *et al*., 2002). Because nocodazole treatment of freshly plated cells does not induce pronounced stress fiber assembly, our results in Figure 7A clearly indicate that the effect of microtubule depolymerization on the formation of extensions indeed reflects their critical involvement in this process rather than secondary effects on the actin cytoskeleton.

Conversely, formation of extensions still occurs after microtubule stabilization by taxol. One interpretation for this result is that microtubule stabilization is an important aspect of the formation of neurite-like extensions. Indeed, a hallmark of neurites is the presence of stable microtubule-associated Glu-tubulin (Paturle-Lafanechere *et al*., 1994). Furthermore, selective polymerization and orientation of stabilized Glu-microtubules has been reported to occur during cell polarization and directional motility (Cook *et al*., 1998).

Analogous to the microtubule bundling that occurs upon assembly of the mitotic spindle in the presence of taxol (Jordan *et al*., 1993), we found that taxol stabilized microtubules can also still be bundled into cytoplasmic extensions in response to ROCK inhibition. However, the pronounced elongation of these Y-27632–induced extensions is blocked by taxol. This indicates that, as one might expect, microtubule dynamics is important for the pronounced elongation of the cytoplasmic extensions. Furthermore, our results indicate that Glu-tubulin–associated microtubule stabilization is not part of the underlying mechanism for formation of the neurite-like extensions. Although induction of neurite-like extensions does involve a pronounced reorientation of microtubules into parallel bundles, this occurs in the absence of Glu-microtubule formation. Rather, Glu-microtubules arise at a later time point, when the extensions and the extensive microtubule bundling have essentially reached completion. Hence, similar to the situation with taxol-treated cells, the emergence of Glu-tubulin presumably reflects a significant degree of microtubule stabilization after their assembly into microtubule bundles. These results therefore suggest that one of the principal initial events driving the formation of these extensions is microtubule reorganization into bundles. Importantly, though, the accumulation of Glu- and acetylated tubulin in the extensions of Y-27632–treated 388-Cbl expressing NIH 3T3 fibroblasts is similar to the accumulation of these posttranslationally modified tubulin isoforms in neurites of PC12 and neuronal cells. The similarity between these cytoplasmic extensions is further highlighted by the resistance of their microtubule components to nocodazole depolymerization. In light of these similarities, it is clear that these extensions can be considered neurite-like, as suggested previously (Hirose *et al*., 1998).

It has been well established that ROCK, one of the principal effectors of Rho (Aspenstrom, 1999), is an important regulator of the actin cytoskeleton. Through its effect on

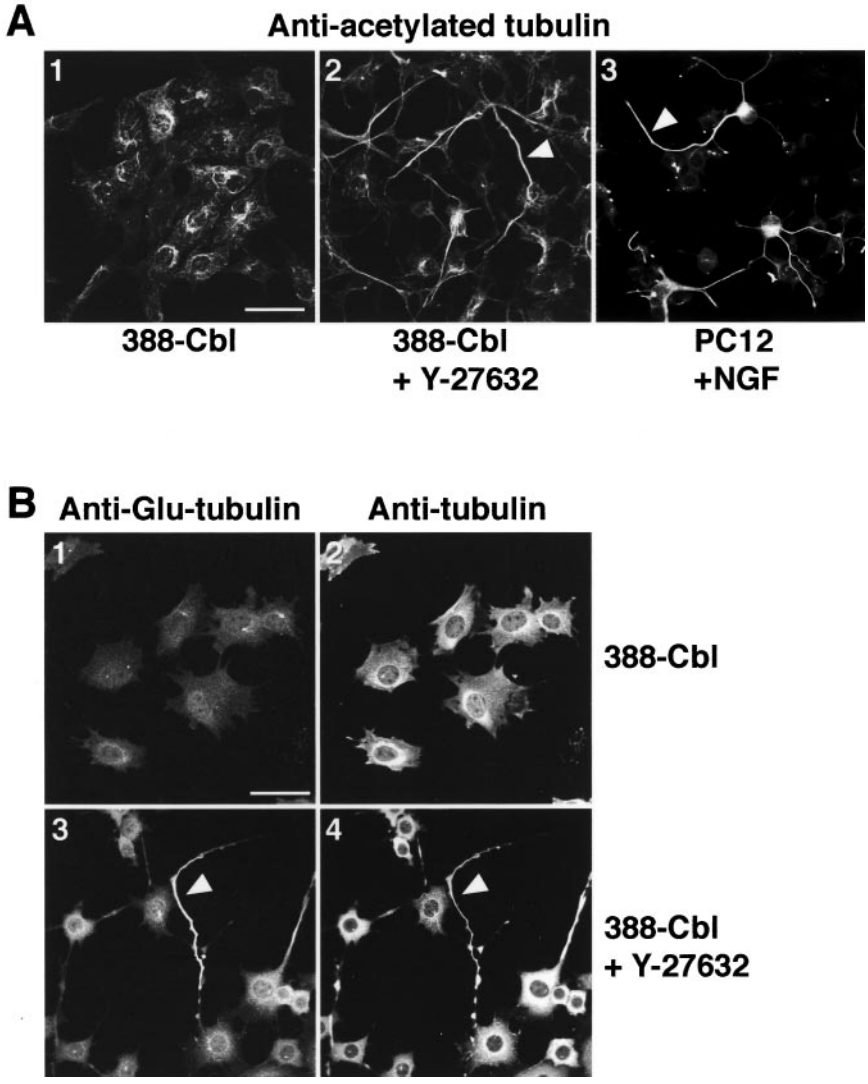

Figure 9. Accumulation of acetylated tubulin and nocodazole-resistant microtubules in Y-27632–induced neurite-like extensions. (A) Confocal immunofluorescence microscopy images of anti-acetylated-tubulin staining of either 388-Cbl–expressing cells replated for 20 h in the absence (1) or presence of Y-27632 (2) or PC12 cells exposed to NGF for 72 h (3). Acetylated tubulin containing microtubule bundles are indicated by the arrowheads. Bar, 50 μm. (B) 388-Cbl–expressing cells were replated for 20 h in the absence (1 and 2) or presence of Y-27632 (3 and 4). Confocal immunofluorescence microscopy images of anti-Glu-tubulin (1 and 3) and anti-β-tubulin (2 and 4) staining were then collected after exposure of the cells to 1 μM nocodazole for 30 min. Glu-tubulin–rich nocodazole-resistant microtubule bundles are indicated by the arrowheads. Bar, 50 μm.

myosin light chain phosphorylation (Kimura *et al*., 1996; Ridley, 1999), and possibly also as a result of its ability to phosphorylate the ezrin/radixin/moesin components of focal adhesion (Matsui *et al*., 1998), ROCK inhibition leads to stress fiber disassembly. ROCK inhibition has also been reported to lead to cell polarization (Hirose *et al*., 1998; Piddini *et al*., 2001; Ward *et al*., 2002), and this effect has been associated with changes to the microtubule cytoskeleton (Hirose *et al*., 1998; Omelchenko *et al*., 2002). Similar to the effect reported here for fibroblasts, ROCK inhibition has recently been shown to induce neurite elongation and branching in hippocampal neurons (Tanaka *et al*., 2002), and rapid neurite formation has also been described for Y-27632–treated N1E-115 cells and cerebellar granule neurons (Hirose *et al*., 1998; Bito *et al*., 2000). It has hence recently been proposed that the cellular mechanisms involved in neuritogenesis may be similar to the polarization and actin dynamics of nonneuronal cells (Da Silva and Dotti, 2002). Our results clearly support this suggestion, although it seems that effects on microtubule organization, rather than changes in actin assembly dynamics, may be critical for polarization and neurite formation.

Although no molecular mechanism has been proposed for the effect of ROCK inhibition on microtubules, it is clear from our results that this response is greatly enhanced in dominant negative Cbl-expressing cells. Cbl itself has also been identified as an important regulator of the cytoskeleton (Krawczyk *et al*., 2000; Scaife and Langdon, 2000; Scaife *et al*., 2003). Indeed, Cbl inhibition is known to lead to increased activation of Rho-family proteins (Krawczyk *et al*., 2000; Scaife *et al*., 2003; Shao *et al*., 2003). The effect of Cbl on T-cell receptor-mediated Cdc42 activation seems to result from altered tyrosine phosphorylation of the guanine nucleotide exchange factor Vav (Bachmaier *et al*., 2000; Chiang *et al*., 2000). Similarly, the pronounced effect of dominant negative Cbl on actin dorsal ruffle formation correlates with an increase in RTK-dependent Rac-activation (Scaife *et al*., 2003). The effect of Cbl on the actin cytoskeleton is therefore fully consistent with its proposed role in attenuation of RTK signaling (Thien and Langdon, 2001). The results presented here demonstrate that the microtubule network is also profoundly affected after activation of the PDGF receptor in 388-Cbl–expressing cells.

The PDGF-induced reorganization of microtubules is also blocked by constitutively active Rho. Furthermore, as described above, a direct block of signaling down stream of Rho, by inhibition of ROCK, faithfully reproduces the same microtubule reorganization as PDGF. It is therefore tempting to speculate that Rho/ROCK inhibition or PDGF stimulation can lead to an equivalent reorganization of microtubules into bundles. However, this does not explain the vastly increased microtubule bundling and formation of neurite-like extensions in 388-Cbl–expressing cells treated by Y-27632 or PDGF. Indeed, the pharmacological inhibition of ROCK can be presumed equal in both wild-type and 388-Cbl–expressing cells, yet the magnitude of the ensuing microtubule rearrangement is very different. This suggests that an additional Cbl-regulated signaling pathway is involved in the pronounced formation of extensions in 388-Cbl–expressing NIH 3T3 cells. Interestingly, δ-catenin has recently been shown to induce neurite elongation in PC12 and primary neuronal cells that is not directly related to Rho/ROCK inhibition (Cruz-Martinez *et al*., 2003). The neuritogenic effect of δ-catenin, which is sensitive to tyrosine phosphorylation by Src kinases, is not affected by dominant negative Rac or Cdc42 constructs. This is reminiscent of the effect of 388-Cbl on NIH 3T3 cells, and it is worth noting that the Cbl-related protein Hakai has been implicated in the stability of cadherin-catenin contact sites (Fujita *et al*., 2002). Clearly though, considerable further investigation will be required to establish whether, and how, Cbl affects δ-catenin and neuritogenesis.

ACKNOWLEDGMENTS

We thank Christine Thien for helpful suggestions, Alan Hall for providing the L63-Rho cDNA construct, Natalie Morin for providing the EGFP-N17-Rac/Cdc42 cDNA constructs, Michiyaka Matsuda for the Crk cDNA construct, Jannie Borst for the NLS-GFP vector, Chandra Kumar for the SCH-51344, Sara Courtneidge for the SU-6656, and Welfide for the Y-27632. We also acknowledge Paul Rigby for assistance with the WA Lotteries Commission confocal microscope. This work was funded by project grant 981649 from the National Health and Medical Research Council (Canberra) and a grant from the Association pour la Recherche sur le Cancer (Paris).

REFERENCES

Andoniou, C.E., Thien, C.B.F., and Langdon, W.Y. (1994). Tumour induction by activated abl involves tyrosine phosphorylation of the product of the *cbl* oncogene. EMBO J. *13*, 4515–4523.

Aspenstrom, P. (1999). Effectors for the Rho GTPases. Curr. Opin. Cell Biol. *11*, 95–102.

Bachmaier, K., Krawczyk, C., Kozieradzki, I., Kong, Y., Sasaki, T., Oliviera-dos-santos, A., Mariathasan, S.D.B., Wakeham, A., Itle, A., *et al.* (2000) Negative regulation of lymphocyte activation and autoimmunity by the molecular adaptor Cbl-b. Nature *403*, 211–216.

Bito, H., Furuyashiki, T., Ishihara, H., Shibasaki, Y., Ohashi, K., Mizuno, K., Maekewa, M., Ishizaki, T., and Narumiya, S. (2000). A critical role for a Rho-associated kinase, p160ROCK in determination of axon outgrowth in mammalian CNS neurons. Neuron *26*, 431–441.

Chiang, Y.J., Kole, H., Brown, K., Naramura, M., Fukuhara, S., Hu, R.J., Kyung, J., Gutkind, J.S., Shevach, E., and Gu, H. (2000). Cbl-b regulates the CD28 dependence of T-cell activation. Nature *403*, 216–220.

Cook, T.A., Nagasaki, T., and Gundersen, G.G. (1998). Rho Guanosine triphosphatase mediates the selective stabilization of microtubules induced by lysophosphatidic acid. J. Cell Biol. *141*, 175–185.

Cruz-Martinez, M., Ochiishi, T., Majewski, M., and Kosik, K. (2003). Dual regulation of neuronal morphogenesis by a δ-catenin-cortactin complex and Rho. J. Cell Biol. *162*, 99–111.

Da Silva, J.S., and Dotti, C.G. (2002). Breaking the neuronal sphere: regulation of the actin cytoskeleton in neuritogenesis. Nat. Rev. Neurosci. *3*, 694–704.

Etienne-Manneville, S., and Hall, A. (2003). Cdc42 regulates GSK-3b and adenomatous polyposis coli to control cell polarity. Nature *421*, 753–756.

Fujita, Y., Krause, G., Scheffner, M., Zechner, D., Molina-Leddy, H.E., Behrens, J., Somer, T., and Birchmaier, W. (2002). Hakai, a c-Cbl-like protein, ubiquinates and induces endocytosis of the E-cadherin complex. Nat. Cell Biol. *4*, 222–231.

Fukata, M., Watanabe, T., Noritake, J., Nakagawa, M., Yamaga, M., Kuroda, S., Matsuura, Y., Iwamatsu, A., Perez, F., and Kaibuchi, K. (2002). Rac 1 and Cdc42 capture microtubules through IQGAP1 and CLIP-170. Cell *109*, 873–885.

Fukata, Y., Oshiro, N., Kinoshita, N., Kawano, Y., Matsuoka, Y., Bennett, V., Matsuura, Y., and Kaibuchi, K. (1999). Phosphorylation of adducin by Rho-kinase plays a crucial role in cell motility. J. Cell Biol. *145*, 347–361.

Gunderson, G.G., and Cook, T.A. (1999). Microtubules and signal transduction. Curr. Opin. Cell Biol. *11*, 81–94.

Hall, A. (1998). Rho GTPases and the cytoskeleton. Science *279*, 509–514.

Hirose, M., Ishizaki, T., Watanabe, N., Uehata, M., Kranenburg, O., Moolenaar, W.H., Matsumura, F., Maekawa, M., Bito, H., and Narumiya, S. (1998). Molecular dissection of the Rho-associated protein kinase (p160ROCK)-regulated neurite remodelling in neuroblastoma N1E-115 cells. J. Cell Biol. *141*, 1625–1636.

Hollenbeck, P. (2001). Cytoskeleton: microtubules get the signal. Curr. Biol. *11*, R820–R823.

Joazeiro, C.A.P., Wing, S., Huang, H.K., Leverson, J.D., and Hunter, T. (1999). The tyrosine kinase negative regulator c-Cbl as a RING-type E2-dependent ubiquitin-protein ligase. Science *286*, 309–312.

Jordan, M.A., Toso, J.R., Trower, D., and Wilson, L. (1993). Mechanism of mitotic block and inhibition of cell proliferatin by taxol at low concentrations. Proc. Natl.Acad. Sci. USA, *90*, 9552–9556.

Kimura, K., Itoh, M., Amano, M., Chihara, K., Fukata, Y., Nakafuku, M., Yamamori, B., Feng, J., Nakano, T., Okawa, K., *et al.* (1996). Regulation of myosin phosphatase by Rho and Rho-associated kinase (Rho-kinase). Science *269*, 221–223.

Krawczyk, C., Bachmaier, K., Sasaki, T., Jones, R.G., S. B., S., D., B., Kozieradzki, I., Ohashi, P.S., Alt, F.W., and Penninger, J.M. (2000). Cbl-b is a negative regulator of receptor clustering and raft aggregation in T cells. Immunity *13*, 463–473.

Krendel, M., Zenke, F.T., and Bokoch, G.M. (2002). Nucleotide exchange factor GEF-H1 mediates cross-talk between microtubules and the actin cytoskeleton. Nat. Cell Biol. *4*, 294–301.

Lim, S.-S., Sammak, P.J., and Borisy, G.G. (1989). Progressive and spatially differentiated stability of microtubules in developing neuronal cells. J. Cell Biol. *109*, 253–263.

Luo, L. (2000). Rho GTPases in neuronal morphogenesis. Nat. Rev. Neurosci. *1*, 173–180.

Marsh, L., and Letourneau, P.C. (1984). Growth of neurites without filopodial or lamellipodial activity in the presence of cytochalasin B. J. Cell Biol. *99*, 2041–2047.

Matsui, T., Maeda, M., Doi, Y., Yonemura, S., Amano, M., Kaibuchi, K., Tsukita, S., and Tsukita, S. (1998). Rho-kinase phosphorylates COOH-terminal threonines of Ezrin/Radixin/Moesin (ERM) proteins and regulates their head-to-tail association. J. Cell Biol. *140*, 647–657.

Nobes, C.D., and Hall, A. (1999). Rho GTPases control polarity, protrusion, and adhesion during cell movement. J. Cell Biol. *144*, 1235–1244.

Omelchenko, T., Vasiliev, J.M., Gelfand, I.M., Feder, H.H., and E. M.B. (2002) Mechanisms of polarization of the shape of fibroblasts and epitheliocytes: separation of the roles of microtubules and Rho-dependent actin-myosin contractility. Proc. Natl. Acad. Sci. USA *99*, 10452–10457.

Palazzo, A.F., Cook, T.A., Alberts, A.S., and Gundersen, G.G. (2001). mDia mediates Rho-regulated formation and orientation of stable microtubules. Nat. Cell Biol. *3*, 723–729.

Paturle-Lafanechere, L.M.M., Trigault, N., Pirollet, F.H.M., and Jod, D. (1994). Accumulation of delta 2-tubulin, a major tubulin variant that cannot be tyrosinated, in neuronal tissues and in stable microtubule assemblies. J. Cell Sci. *107*, 1529–1543.

Piddini, E., Schmid, J., de Martin, R., and Dotti, C.G. (2001). The Ras-like GTPase Gem is involved in cell shape remodelling and interacts with the novel kinesin-like protein KIF9. EMBO J. *20*, 4076–4087.

Ridley, A. (1999). Stress fibers take shape. Nat. Cell Biol. *1*, E64–E65.

Rodriguez-Viciana, P., Warne, P.H., Kwaja, A., Marte, B.M., Pappin, D., Das, P., Waterfield, M., Ridley, A., and Downward, J. (1997). Role of phosphoinositide 3-OH kinase in cell transformation and control of the actin cytoskeleton by ras. Cell *89*, 457–467.

Sander, E.E., ten Klooster, J.P., van Delft, S., van der Kammen, R.A., and Collard, J.G. (1999). Rac downregulates Rho activity: reciprocal balance between both G.T.Pases determines cellular morphology and migratory behavior. J. Cell Biol. *147*, 1009–1021.

Scaife, R.M., Courtneidge, S.A., and Langdon, W.Y. (2003). The multi-adaptor proto-oncoprotein Cbl is a key regulator of actin assembly and Rac. J. Cell Sci. *116*, 463–473.

Scaife, R.M., and Langdon, W.Y. (2000). c-Cbl localizes to actin lamellae and regulates lamellipodia formation and cell morphology. J. Cell Sci. *113*, 215–226.

Schaefer, A.W., Kabir, N., and Forscher, P. (2002). Filopodia and actin arcs guide the assembly and transport of two populations of microtubules with unique dynamic parameters in neuronal growth cones. J. Cell Biol. *158*, 139–152.

Shao, Y., Elly, C., and Liu, Y.-C. (2003). Negative regulation of Rap1 activation by the Cbl E3 ubiquitin ligase. EMBO Rep. *4*, 425–431.

Tanaka, H., Yamashita, T., Asada, M., Mizutani, S., Yoshikawa, H. and M.T. (2002) Cytoplasmic p21Cip1/WAF1 regulates neurite remodelling by inhibiting Rho-kinase activity. J. Cell Biol. *158*, 321–329.

Tanaka, S., Hattori, S., Kurata, T., Nagashima, K., Fukui, Y., Nakamura, S., and Matsuda, M. (1993). Both the SH2 and SH3 domains of human CRK protein are required for neuronal differentiation of PC12 cells. Mol. Cell. Biol. *13*, 4409–4415.

Thien, C.B.F., and Langdon, W.Y. (2001). Cbl: many adaptations to regulate protein tyrosine kinases. Nat. Rev. Mol. Cell. Biol. *2*, 294–305.

Thien, C.B.F., Scaife, R.M., Papadimitriou, J.M., Murphy, M.A., Bowtell, D.L., and Langdon, W.Y. (2003). A mouse with a loss-of-function mutation in the c-Cbl TKB domain shows perturbed thymocyte signalling without enhancing the activity of the ZAP-70 tyrosine kinase. J. Exp. Med. *197*, 503–513.

Tsuji, T., Ishizaki, T., Okamoto, M., Higashida, C., Kimura, K., Furuyashiki, T., Arakawa, Y., Birge, R.B., Nakamoto, T., Hirai, H., *et al.* (2002). ROCK and mDia antagonize in Rho-dependent Rac activation in Swiss 3T3 fibroblasts. J. Cell Biol. *157*, 819–830.

Ward, Y., Yap, S.-F., Ravichandran, V., Matsumura, F., Ito, M., Spinelli, B. and K.K. (2002) The GTP binding proteins Gem and Rad are negative regulators of the Rho-Rho kinase pathway. J. Cell Biol. *157*, 291–302.

Wittman, T., and Waterman-Storer, C.M. (2001). Cell motility: can Rho GTPases and microtubules point the way. J. Cell Sci. *114*, 3795–3803.

Woodring, P., Litwack, E., O'Leary, D., Lucero, G., Wang, J., and Hunter, T. (2002). Modulation of the F-actin cytoskeleton by c-Abl tyrosine kinase in cell spreading and neurite extension. J. Cell Biol. *156*, 879–892.

Zhou, F.-Q., Waterman-Storer, C.M., and Cohan, C.S. (2002). Focal loss of actin bundles causes microtubule redistribution and growth cone turning. J. Cell Biol. *157*, 839–849.